(11) T. Kawauchi and Y. Ishida, private communication.
(12) R. E. Naylor and S. W. Lasoski, *J. Polym. Sci.*, **44**, 1 (1960).
(13) C. W. Wilson and E. R. Santee, *J. Polym. Sci., Part A*, **1**, 1305 (1963).
(14) F. C. Wilson and H. W. Starkweather, Jr., *J. Polym. Sci., Polym. Phys. Ed.*, **11**, 919 (1973).
(15) M. Modena, C. Garbuglio, and M. Ragazzini, *J. Polym. Sci., Part B*, **10**, 153 (1972).
(16) W. W. Doll and J. B. Lando, *J. Macromol. Sci., Phys.*, **2**, 205 (1968).
(17) G. Zerbi, *Pure Appl. Chem.*, **26**, 499 (1971).
(18) R. C. Newman, "Infra-red Studies of Crystal Defects," Taylor and Francis, London, 1973.
(19) J. F. Rabolt and K. W. Johnson, *J. Chem. Phys.*, **59**, 3710 (1973).

Nuclear Magnetic Resonance Relaxation and the Microbrownian Motion in Polymers. Local and Collective Motions and Their Viscosity Dependence

G. Hermann and G. Weill*

Centre de Recherches sur les Macromolécules CNRS, Strasbourg, France.
Received July 19, 1974

ABSTRACT: The loss of orientation memory for a vector linked to a polymer chain is expected to present a fast initial decay corresponding to fast local jumps with a long tail corresponding to diffusive cooperative motions. An analysis of the nuclear relaxation times T_1 and T_2 in solvents of high viscosity where the extreme narrowing condition is not fulfilled may help to separate fast and slow processes. Such an analysis is carried out for poly(oxymethylene) in hexafluoro-2-propanol. The results seem to indicate that both slow and fast processes are linearly dependent on the viscosity, a result of importance for the concept of internal viscosity.

The low-frequency, long-wavelength modes of a polymer chain are adequately described by models derived from the Gaussian subchain model of Rouse.[1] Since in these models the exchange between different subchain conformations corresponding to a given end-to-end vector is supposed to be infinitely rapid, they completely neglect the high-frequency part of the spectrum. Dissipative processes related to the motion inside of a subchain can, however, be taken into account by the introduction of a phenomenological "internal viscosity" parameter.[2] New approaches in the description of polymer dynamics, starting from elementary local motions, have followed the initial work of Verdier and Stockmayer on a cubic lattice.[3-5] They all give the Rouse spectrum in the low-frequency limit, a consequence of the diffusive nature of the fluctuations,[6] but the high-frequency part is very dependent upon the special features of the model. The viscosity dependence of the probability of an elementary jump is of particular interest[7] in connection with the corresponding dependence of the internal viscosity.

Experimental techniques specially adapted to the study of fast movements, such as the dielectric dispersion of chains with a transverse component of the electric moment,[8] fluorescence polarization,[9] line-shape analysis of the paramagnetic resonance of spin labels,[10] and nuclear magnetic resonance,[11] have been used with polymer chains. The response of the chain, in the time or frequency domain, is in all cases related to one autocorrelation function for the rotatory motion of a well defined local molecular unit. But in most cases experiments cover only a limited range of time and frequency and the results can be interpreted assuming a single exponential decay of the autocorrelation function, all fast movements compared to the range of time under study being represented by an instantaneous decay of the autocorrelation function from 1 to a smaller value. This is particularly evident for the polarization of fluorescence where it comes to assume a smaller fundamental polarization. But then the variation of the calculated correlation time with temperature and viscosity will incorporate the approximations made in the choice of the autocorrelation function.[12]

For a model chain in which elementary jumps are supposed to be the exchange of orientation of bonds $i - 1$ and $i + 1$ on a tetrahedral lattice, the complete autocorrelation function has been calculated[13] and found identical with that calculated by Hunt and Powles[14] for the one-dimensional diffusion of a defect, with a fast initial decay and a long $t^{-1/2}$ tail. One can expect this to be a quite general behavior in polymer chains, most of the orientation memory being lost in the first local motions, while a complete loss requires long cooperative motions of the chain. These are required since energetically highly unfavorable conformations, like g^+g^-, generally limit the diffusion by the three bonds mechanism. The relative independence of fast and slow processes finds supports in the calculations of Helfand,[15] who consider the motion of a few segments with Rouse chains at the extremities.

As part of an effort to characterize from an experimental point of view these slow and fast processes we present in this work an nmr relaxation study on simple polymers in solution, where special attention has been paid to the information which can be derived from differences between T_1 and T_2 that is, when the extreme narrowing limit is not completely reached, from the use of measurements on several nuclei (^1H, ^2H, and ^{13}C), and from the viscosity dependence of the relaxation times.

I. Nmr Relaxation Times and Autocorrelation Functions

In the case under study, the nmr relaxation times are governed by the rotation through the autocorrelation function of the second spherical harmonic $P_2(t) = \langle 3\cos^2\theta(t) - 1\rangle/2$ where $\theta(t)$ is the angle of a vector linked to the polymer segment at time t with its original direction at time 0. This vector will be the vector joining two protons, or one proton to the C atom in the case of the dipolar relaxation of the proton and ^{13}C of a CH_2 group, or the axis of the electric field gradient in the case of the quadrupolar relaxation of D.

The expressions for the spin–lattice T_1 and spin–spin T_2 relaxation times are given in the three cases by[16] (a) dipolar relaxation of two ½ identical spins

$$\frac{1}{T_1} = \frac{3}{40}\frac{\gamma^4\hbar^2}{r^6}[2J(\omega) + 8J(2\omega)] \quad (1)$$

$$\frac{1}{T_2} = \frac{3}{40}\frac{\gamma^4\hbar^2}{r^6}[3J(0) + 5J(\omega) + 2J(2\omega)] \quad (2)$$

(b) dipolar relaxation of two ½ unlike spins under saturation of S

$$\frac{1}{T_1^I} =$$

$$\frac{1}{20}\frac{\gamma_I^2\gamma_S^2\hbar^2}{r^6}[J(\omega_I - \omega_S) + 3J(\omega_I) + 6J(\omega_I + \omega_S)] \quad (3)$$

$$\frac{1}{T_2^I} = \frac{1}{40}\frac{\gamma_I^2\gamma_S^2\hbar^2}{r^6}[J(\omega_I - \omega_S) + 3J(\omega_I) + 6J(\omega_I + \omega_S) + 4J(0) + 6J(\omega_S)] \quad (4)$$

(c) quadripolar relaxation of one spin 1 nucleus

$$\frac{1}{T_1} = \frac{3}{80}\left(1 + \frac{\eta^2}{3}\right)(e^2qQ)^2[J(\omega) + 4J(2\omega)] \quad (5)$$

$$\frac{1}{T_2} = \frac{1}{160}\left(1 + \frac{\eta^2}{3}\right)(e^2qQ)^2[9J(0) + 15J(\omega) + 6J(2\omega)] \quad (6)$$

where γ is the gyromagnetic ratio, r is the distance between the nuclei, $J(\omega)$ is the reduced spectral density, Fourier transform of $P_2(t)$, ω_I and ω_S are the Larmor frequencies, (e^2qQ) is the quadrupolar coupling constant, and η is the asymetry parameter.

For an exponential autocorrelation function $J(\omega) = 2\tau/(1 + \omega^2\tau^2)$. In the case of a more complicated autocorrelation function one must be aware of the fact that the measurements of T_1 and T_2 should extend over an extremely large range of ω and/or τ. If one uses a spectrum of correlation time, that is represents the autocorrelation function on an exponential basis, with τ values between τ_{min} and τ_{max}, this range should extend from $\omega\tau_{max} \ll 1$ up to $\omega\tau_{min} \gg 1$. This can be made for nonselective relaxation studies in solids where in addition to T_1 and T_2, relaxation times in the rotatory frame $T_{1\rho}$ are equivalent to low-frequency measurements with the sensitivity of the high frequencies.[17] But then one gets generally an average of the different chemically nonequivalent nuclei of a given type. Selective relaxation measurements, as needed when studying a solution in solvents containing the same nuclei, are limited to the neighborhood of the extreme narrowing condition $\omega\tau \ll 1$, and the information is restricted to a small frequency or τ values excursion below $\omega\tau = 1$. In this region T_2 begins to be smaller than T_1 while remaining sufficiently large so that the different signals do not overlap. This is equivalent to a study of a restricted part of the autocorrelation function in the time domain and it is therefore evident that it will be possible to represent it by a series of discrete correlation times or by an analytical spectrum defined by two parameters. The simplest molecular model of motion leading to a sum of exponentials is an anisotropic movement, such as that of a symmetrical ellipsoid with two rotatory diffusion constants R_1 and R_2.

In this case[18]

$$J(\omega) = A\frac{2\tau_A}{1 + \omega^2\tau_A^2} + B\frac{2\tau_B}{1 + \omega^2\tau_B^2} + C\frac{2\tau_C}{1 + \omega^2\tau_C^2} \quad (7)$$

where $\tau_A^{-1} = 6R_2$, $A = \frac{1}{4}(3\cos^2\alpha - 1)^2$, $\tau_B^{-1} = R_1 + 5R_2$, $B = 3\cos^2\alpha(1 - \cos^2\alpha)$, $\tau_C^{-1} = 4R_1 + 2R_2$, $C = 3((\cos^2\alpha - 1)/2)^2$, and α is the angle of the vector of interest with the symmetry axis of the ellipsoid. Since we do not expect that our results could be sufficiently accurate to describe the autocorrelation function by more than three exponentials in a restricted time domain, this model will cover, by an appropriate choice of $\cos^2\alpha$ and of $\sigma = R_1/R_2$, nearly all possible cases. We have therefore used it in the interpretation of our experimental results. This in no way means that we really believe that the motion of an element in a chain is that of an ellipsoid but it is a good representation for our mixture of fast processes which do not completely average out the dipolar interaction and slower processes necessary for a complete loss of the orientation memory.

It will be possible afterwards in the time domain to compare the sum of exponentials to the autocorrelation functions obtained with more sophisticated models, which happen to be much less tractable. In particular, the defect diffusion model of Hunt and Powles[14] has

$$P_2(t) = e^{+(t/\tau)}\left(erfc\left(\frac{t}{\tau}\right)^{1/2}\right) \quad (8)$$

$$J(\omega) = \frac{2\omega^{-1/2}\tau^{1/2}}{1 + \omega\tau + (2\omega\tau)^{1/2}} \quad (9)$$

so that it cannot be used for the comparison of T_1 and T_2 without introducing some arbitrary faster decrease of $P_2(t)$ at long times to get a finite $J(0)$.

Some supplementary information can be obtained eventually with ^{13}C nmr from the nuclear Overhauser enhancement (NOE). This is given under conditions of complete decoupling and assuming that the dipolar interaction between C and H is the only mechanism of ^{13}C relaxation by[19]

$$\text{NOE} = 1 + \frac{\gamma_H}{\gamma_C}\frac{-J(\omega_H - \omega_C) + 6J(\omega_H + \omega_C)}{J(\omega_H - \omega_C) + 3J(\omega_C) + 6J(\omega_H + \omega_C)} \quad (10)$$

with a maximum value of 2.976.

II. Experimental Section

Selective relaxation measurements of T_1 have been performed for the proton by a fast adiabatic passage followed by sampling,[20] with an automated sequence built into a Varian HA-100 high resolution nmr spectrometer.[21] Measurements can be carried down to $T_1 = 0.1$ sec. T_2 was calculated from line width, taking into account the instrumental residual inhomogeneity as measured on solvent lines, both measurements being carried out at sufficiently low radiofrequency fields H_1 to avoid any saturation broadening. On the other hand, progressive saturation studies were carried out in a deliberately inhomogeneous field so that the maximum of the signal is given by

$$v = KH_1/(1 + \gamma^2H_1^2T_1T_2)^{1/2}$$

The product T_1T_2 has been obtained from the linear plot of $(v/H_1)^{-2}$ *vs.* H_1^2. A careful calibration of H_1 available at the center band for the determination of the conditions of fast adiabatic passage has been performed by the side-band technique of Freeman[20] and used to measure the water T_1T_2 in a solution of SO_4Cu. This in turn has been used to measure H_1 at the side band as a function of the modulation index β. The absorption signal follows quite satisfactorily the theoretical relation[20]

$$v \propto \frac{[J_0(\beta) - J_2(\beta)]J_1(\beta)H_1}{1 + [\Delta\omega + \omega_m T_2]^2 + [\gamma J_1(\beta)H_1]^2T_1T_2}$$

where J_0, J_1, J_2 are the Bessel functions of respectively zero, first, and second kind. Reliability of the different experiments down to values of $T_1 \sim 0.1$ sec has been checked using Cu^{2+} doped water samples.

^{13}C relaxation measurements under complete decoupling and NOE measurements have been performed on a Varian XL 100 FT instrument. ^{13}C Overhauser enhancement has been calculated from the comparison of the signal area under no or complete proton decoupling with a rather low precision (±0.3) at temperatures other than the magnet temperature (~30°).

Deuterium quadrupolar relaxation times T_{1q} have been measured indirectly from the analysis of the J coupled proton signal in a CHD unit. The signal is expected to go from a single line for $T_q \ll J_{HD}^{-1}$ to a triplet with a spacing equal to J_{HD} for $T_q \gg J_{HD}^{-1}$.

Table I
Relaxation Times of ^1H (100 MHz) and ^{13}C (25.2 MHz) for POM in HFIP

	Temp, °C								
	−20	−10	0	10	20	30	45	62	73
$T_{1,H}$	0.105 ± 0.005	0.125 ± 0.005	0.145 ± 0.005	0.21 ± 0.01	0.31 ± 0.01	0.46 ± 0.02	0.72 ± 0.02	1.08 ± 0.03	1.36 ± 0.03
$T_{2,H}$	0.055 ± 0.005	0.075 ± 0.005	0.085 ± 0.005	0.15 ± 0.01	0.25 ± 0.01	0.45 ± 0.02			
$T_{1,^{13}C}$		0.068 ± 0.005	0.096 ± 0.005			0.30 ± 0.02			
$T_{2,^{13}C}$		0.060 ± 0.005	0.094 ± 0.005			0.30 ± 0.02			
NOE		3 ± 0.3	3 ± 0.3			3 ± 0.3			

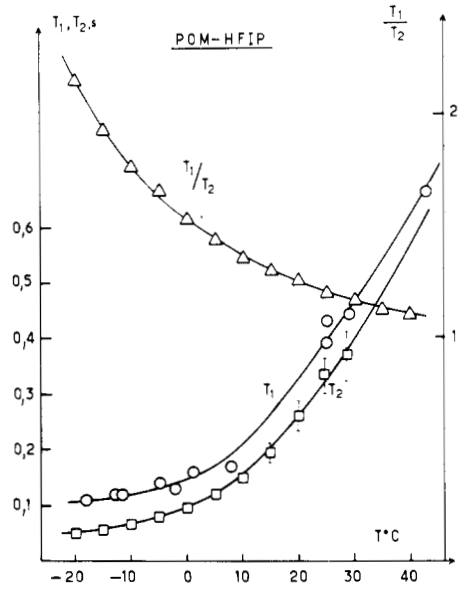

Figure 1. T_1 and T_2 for POM in HFIP.

For $J_{HD}T_q \sim 1$, T_q has been obtained either from the line width $\delta\nu_{1/2}$ (taking into account the residual inhomogeneity line width $\delta\nu_{o1/2}$)

$$\delta\nu_{1/2} - \delta\nu_{o1/2} = 6T_q J_{HD}^2$$

or from a complete calculation of the line shape using a program written by Kintzinger[22] where a phenomenological inhomogeneity broadening can be introduced.

Temperature was controlled through the standard Varian nitrogen flow accessory and was measured from the splitting of a glycerol sample.

III. Results in Polyoxymethylene and Its Monodeuterated Analog

Polyoxymethylene $(O\text{-}CH_2)_n$ is very well suited for the nmr relaxation study since all protons are equivalent and the distance between geminal protons (1.78 Å) is sufficiently smaller than any other distance between protons belonging to neighboring units in the helical conformation of lowest energy ($g^+g^+g^+ \ldots$ or $g^-g^-g^- \ldots$) as well as in the most probable defects ($g^{++}g^-, g^{++}g^+, g^{--}g^-$), the chain being described in the isomeric rotamer model as a succession of g^+ or g^- helical segments articulated on a trans segment.[23] The polymers studied were one sample of a commercial polymer (DELRIN 500 mol wt = 75,000) and one sample of lower molecular weight (mol wt = 23,000) provided by Professor Walter Stockmayer. No differences were found between these samples. The monodeuterated analog is commercially available (Merck Sharp Dohme of Canada) allowing parallel measurements to be carried on H, D, and ^{13}C.

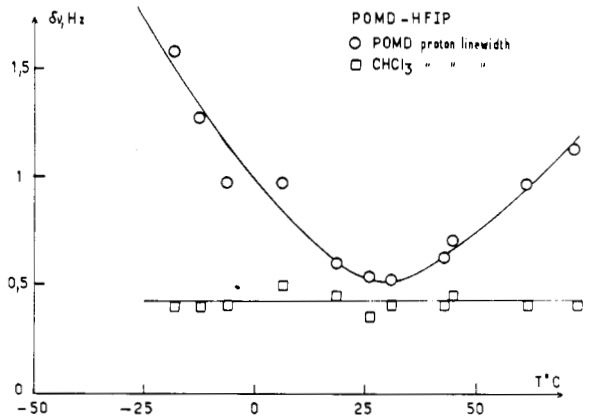

Figure 2. Proton line width as a function of temperature for monodeuterated POM in HFIP.

Poly(oxymethylene) (POM) has, however, two drawbacks. (a) There are very few solvents for this polymer and none of these are deuterated. Hexafluoro-2-propanol (HFIP) has been found the most suitable due to a low temperature of crystallization and a rather high viscosity. As the viscosity of HFIP as a function of temperature was not reported, we have measured it together with densities at several temperatures yielding an activation energy for viscosity of 7.7 kcal/mol. (b) The polymer can undergo a rapid depolymerization into formaldehyde above room temperature. DELRIN is stabilized by end group methylation but care must be exercized when working above room temperature. Moreover, we have found that degassing of the solution favors the depolymerization. No removal of oxygen has therefore been possible but we have determined using pure solvent that O_2 makes a negligible contribution to T_1 (3.65 sec without O_2 against 3.40 sec without degassing).

All measurements have been performed on solutions between 1 and 3%, over which range no variation with the concentration has been observed. T_1 and T_2 observed for ^1H and ^{13}C together with NOE of ^{13}C are reported in Table I and Figure 1.

The signal of the proton in the monodeuterated compound does not show any splitting at the highest temperature we have been able to study. The line width represented in Figure 2 shows, however, that, while below 25° the line width decreases with temperature, due to the normal increase in T_2 with the mobility, the line width increases again above 25° due to the HD coupling. Taking $J_{HD} = (\gamma_D/\gamma_H)J_{HHgem} \sim 2.2$ Hz, T_{1q} has been calculated using the two above mentioned methods leading to the values of Table II.

Another measurement of T_{1q} could in principle be obtained from the J coupled ^{13}C signal, which should be more

Table II
Quadrupolar Relaxation Time T_{1q} of D in $(CHD\text{-}O)_n$ in HFIP from Proton Line Shape Analysis

	Temp, °C		
T_{1q}	45	62	73
From line width	11×10^{-3}	19×10^{-3}	26×10^{-3}
From line shape	$14 \pm 2 \times 10^{-3}$	$19 \pm 3 \times 10^{-3}$	$21 \pm 3 \times 10^{-3}$

broadened due to the high J_{CD} coupling constant. However, we have not been able to use this method due to the degradation of the polymer at elevated temperatures during the long accumulation time necessary for ^{13}C FT spectroscopy of a rather broad line.

IV. Discussion

It is clear, considering the values of T_1/T_2 above the T_1 minimum in Figure 2, that the proton relaxation cannot be satisfactorily described in terms of a simple isotropic motion of a CH_2 unit. For such a model one calculates $T_{1\,min} = 0.082$ sec at $\omega\tau = 0.616$ with $T_1/T_2 = 1.6$. As pointed out before, the contribution of the dipolar interaction between protons of neighboring carbon should not contribute appreciably to the relaxation process. Indeed the factor $1/r_6$, which is 307×10^{-4} Å^{-6} for the two geminal protons, becomes 16×10^{-4} Å^{-6} in the most favored g^+g^+ conformation and even smaller for other local conformations with an exception of the g^+g^- conformation which is for this very reason strongly energetically disfavored due to van der Waals repulsion.

Intermolecular dipolar interaction with solvent nuclei has also been neglected. We have checked with the more soluble polymer poly(oxyethylene) in dimethylformamide (low viscosity, high T_1) and ethylene glycol (high viscosity, low T_1) that the results were unaffected by the use of protonated or deuterated solvent; the high T_1 values observed for the proton of the monodeuterated sample also precludes a sizable contribution from polymer solvent dipolar interaction.

Therefore we have used the geminal H–H distance in relation 1 and 2 to calculate theoretical curves of $T_{1\,min}/T_1$ as a function of T_1/T_2 using the spectral density in (7) with different values of cos α and σ. Starting from the value of $T_{1\,min}$ calculated for the isotropic case ($\sigma = 1$) the experimental values have been reported on a network of theoretical curves (Figure 3). Several "trial" values of cos α and σ can then be selected from a first comparison of the experimental points with the theoretical curves. The value of $T_{1\,min}$ is then recalculated and the new set of points is compared to the network of curves. A satisfactory agreement is very rapidly reached for cos $\alpha = 0.40$ and $\sigma = 40$.

Once again we recall that the geometrical significance of these numbers should not be taken seriously. They just represent a way to use a given sum of three exponentials for the autocorrelation function which with these values become

$$P_2(t) = 0.529e^{-t/\tau_C} + 0.403e^{-t/\tau_B} + 0.0676e^{-t/\tau_A}$$

with $\tau_B = 3.6\tau_C$ and $\tau_A = 27\tau_C$.

Inserting these coefficients into relation 7 we have calculated from T_1 at each temperature the values of τ_A, τ_B, and τ_C listed in Table III together with the value τ_{iso} that one would calculate assuming an isotropic reorientation.

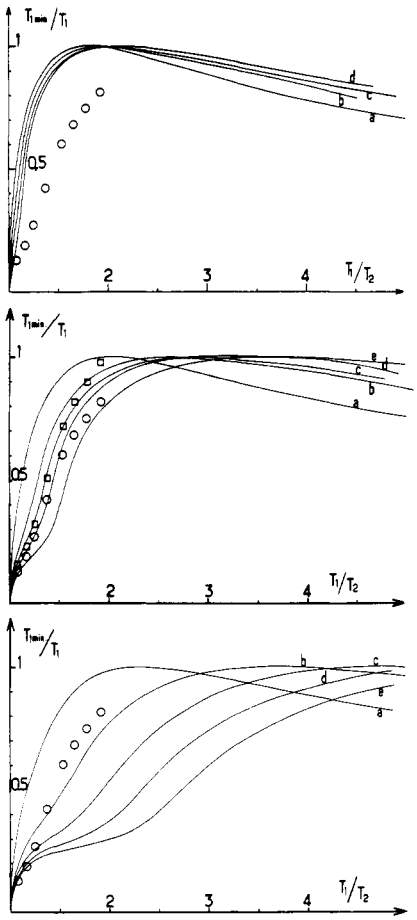

Figure 3. A theoretical network of $T_{1\,min}/T_1$ *vs.* T_1/T_2 curves. For the anisotropic model: (top) cos $\alpha = 0.50$, σ = (a) 11, (b) 31, (c) 51, (d) 71; (middle) cos $\alpha = 0.30$, σ = (a) 11, (b) 31, (c) 51, (d) 71, (e)91; (bottom) cos $\alpha = 0.40$, σ = (a) 11, (b) 31, (c) 41, (d) 51, (e) 71. ○ corresponds to experimental points with a tentative $T_{1\,min}$. ◘ corresponds to the iterated experimental results (see text).

We have used the values of τ in Table III to recalculate the values of T_1 and T_2 and of the NOE of ^{13}C in the high-viscosity range as well as the T_{1q} of deuterium in the low-viscosity range using a standard quadrupolar coupling constant of 170 kHz and an asymetry parameter $\eta = 0$. The results are given in Tables IV and V.

They imply a more isotropic movement for the relaxation of ^{13}C and a more anisotropic movement for the relaxation of deuterium. This result is puzzling since the axis of the field gradient is supposed to be along the C–H bond. At this point no explanation can be offered and direct measurements of T_1 on ^2H are needed.

It is, however, interesting to compare the plots of log $1/T_1$ as a function of $1/T$ or of log η with the corresponding plots for τ_A (Figures 4 and 5).

The plots of T_1 present a curvature in the low-temperature–high-viscosity range. This is due to the fact that in this region $\omega_A\tau_A > 1$ so that the A term in relation 7 starts to decrease. The plots of τ do not present such a curvature (the slight deviation at high T_1 and low τ can be due to the influence of oxygen at high T_1). The log τ–log η results are compatible with a slope 1 and the energy of activation calculated from the $1/T$ plot gives 8 ± 3 kcal/mol to be compared to the value of 7.7 kcal/mol for the viscosity.

This strongly suggests that all fast and slow correlation times have the same proportionality to the solvent viscosi-

Table III
Correlation Times Calculated from T_1 in the Anisotropic and Isotropic Models

	Temp, °C								
	−20	−10	0	10	20	30	45	62	73
T_1, sec	0.105	0.125	0.145	0.210	0.310	0.46	0.72	1.08	1.36
τ_A, 10^{-10} sec	117	58	42	24	12.5	7.3	4.2	2.5	2.0
τ_B, 10^{-10} sec	14.6	7.7	5.6	3.5	1.7	1.0	0.55	0.33	0.26
τ_C, 10^{-10} sec	4.3	2.15	1.55	0.50	0.46	0.27	0.15	0.093	0.074
τ_{is}, 10^{-10} sec	4.1	3.3	2.8	2.0	1.20	0.80	0.51	0.35	0.28
η_{C_P}	18	9.7	5.6	3.55	2.15	1.40	0.77	0.40	0.27

Table IV
Comparison of the Experimental and Calculated Values for ^{13}C

	Anisotropic model			Isotropic model			Experiment		
Temp, °C	T_1	T_2	NOE	T_1	T_2	NOE	T_1	T_2	NOE
−10	0.053	0.47	2.52	0.073	0.070	2.95	0.068	0.060	3 ± 0.3
0	0.066	0.060	2.47	0.085	0.083	2.96	0.096	0.094	3 ± 0.3
30	0.24	0.24	2.88	0.30	0.30	2.97	0.30	0.30	3 ± 0.3

Table V
Comparison of the Experimental and Calculated Values for Deuterium Quadrupolar Relaxation Times T_{1q}

Temp, °C	Anisotropic model	Isotropic model	Experiment
45	39×10^{-3}	45×10^{-3}	14×10^{-3}
62	64.8×10^{-3}	66×10^{-3}	19
73	81×10^{-3}	83×10^{-3}	21

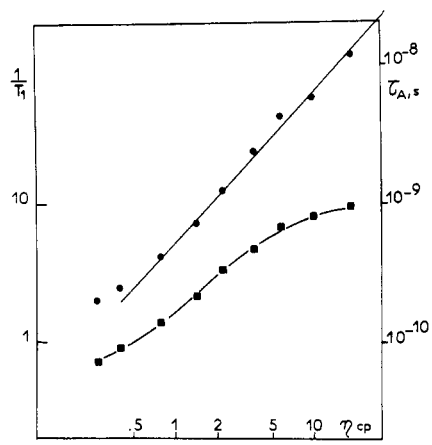

Figure 4. Log $1/T_1$ (■) and log τ (●) as a function of log η.

ty. In fact, this was an assumption in our derivation of the autocorrelation function from an anisotropic model with σ constant and the detection of possible deviations would require a very careful study of T_1 and T_2 for several polymers in solvents of high viscosity. A qualitative preliminary result for poly(oxyethylene) (PEO) in *p*-chlorophenol (*p*-CP) as a function of temperature seems, however, in favor of this proportionality. A plot of $1/T_1$ as function of viscosity is given in Figure 6 together with results obtained by Liu[24] at 60 MHz in a series of halogenated paraffins. The shape of the curve is very well explained considering the decrease of the A term ($\omega\tau_A > 1$) while the B and C terms continue to increase. Analysis of the difference between T_1 and T_2 in the high-viscosity range leads for PEO in *p*-CP to $\cos\alpha = 0.30$ and $\sigma = 40$.

Our sum of exponentials with extreme correlation times

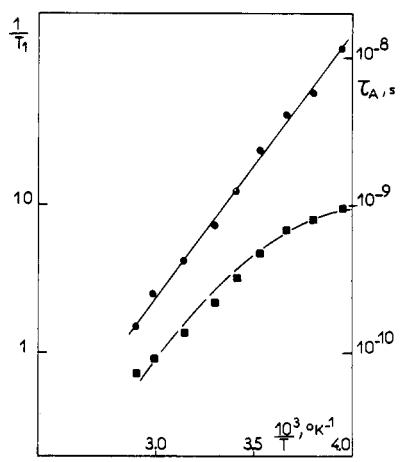

Figure 5. Log $1/T_1$ (■) and log τ(●) as a function of $1/T$.

in a ratio of ~30 can be compared with the theoretical autocorrelation function 8. Figure 7 has been drawn assimilating τ to τ_c. It is clearly seen that the experimental autocorrelation function decreases slightly more slowly at short times but much more rapidly at long times. τ_c can be taken as characteristic of the local process while τ_A should be compared to the Zimm–Rouse relaxation time τ_p for the smallest Gaussian chain, that is of mass m corresponding to 10 to 20 statistical elements. The relation with the longest relaxation time as calculated from the intrinsic viscosity $\tau_1 = m\eta_s[\eta_0]/2.36kT$ can only lead, due to excluded volume and hydrodynamic interaction problems, to an order of magnitude of 10^{-6} η_s, which is higher than our τ_A values.

The analysis of the chain mobility in terms of fast and slow processes shows that one must be very cautions when analyzing nmr relaxation results at a single temperature and viscosity.

Allerhand and Hailstone[25] have recently claimed that the identity of the ^{13}C relaxation times of the phenyl and backbone CH carbons of polystyrene in tetrachloroethylene at 44° implies that the phenyl ring has no fast movements around its bond to the main chain, whereas free rotation would indeed give rise in this case to a much larger T_1. For phenyl protons, it is difficult to exclude fast oscillations from measurements in the extreme narrowing re-

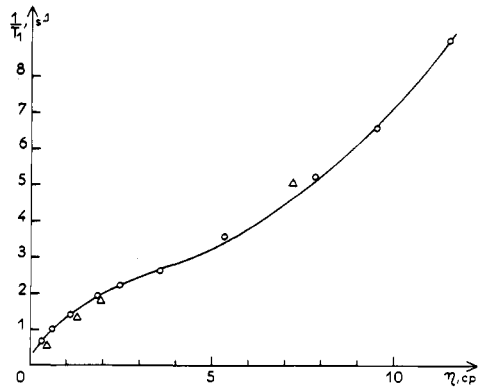

Figure 6. $1/T_1$ as a function of solvent viscosity for PEO in *p*-CP at several temperatures (O) and in halogenated paraffins (Δ results of Liu[24] at 50 MHz).

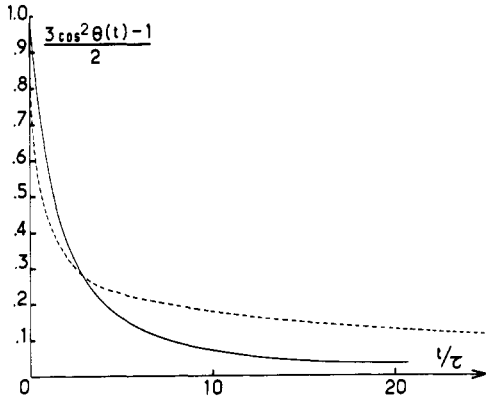

Figure 7. Experimental (—) and theoretical (- - -) (relation 8) autocorrelation function.

gion. Approximately equal values for $\Sigma A_i \tau_i$ (relation 7) may not reflect large differences in the initial part of the autocorrelation, which may become more apparent if one works in conditions where the extreme narrowing condition is not fulfilled.

Schaefer[26] has fitted the ^{13}C values of T_1, T_2, and NOE at one high temperature for polystyrene in *o*-dichlorobenzene, solid polybutadiene, and polyisoprene (all outside of the extreme narrowing region) with a log $-\kappa^2$ distribution of correlation times. Smaller average τ are associated with broader distributions. While the author correctly points out that this might be due to the relative role of fast local and slow cooperative processes, a study of the distribution as a function of the viscosity and temperature could enable one to separate clearly the role of the two processes in a way similar to that used in this work.

Undoubtly, a comparison between the flexibilities of different polymers requires a clear separation of both types of processes. A clear understanding of the motion of a single chain is needed to appreciate the role of constraints, like physical entanglements, in the dynamics of solid polymers.[27]

References and Notes

(1) P. A. Rouse, *J. Chem. Phys.*, **21**, 1272 (1953).
(2) R. Cerf, *Advan. Polym. Sci.*, 382 (1959).
(3) P. H. Verdier and W. H. Stockmayer, *J. Chem. Phys.*, **36**, 229 (1962).
(4) E. Dubois Violette, F. Geny, L. Monnerie, and O. Parod, *J. Chim. Phys. Physiochim. Biol.*, **66**, 1865 (1969).
(5) K. Iwata, *J. Chem. Phys.*, **54**, 12, 1570 (1971).
(6) P. G. de Gennes, *Physics (Long Island City, N. Y.)*, **3**, 37 (1967).
(7) R. Cerf, *Chem. Phys. Lett.*, **24**, 317 (1974).
(8) B. Baysal, B. A. Lowry, H. Yu, and W. H. Stockmayer, "Dielectric Properties of Polymers," F. E. Karasz, Ed., Plenum Press, New York, N. Y., 1972.
(9) P. Wahl, G. Meyer, and J. Parrod, *Eur. Polym. J.*, **6**, 585 (1970).
(10) A. T. Bullick, J. H. Butterworth, and G. C. Cameron, *Eur. Polym. J.*, **7**, 445 (1971).
(11) K. J. Liu and R. Ullmann, *J. Chem. Phys.*, **48**, 1158 (1968).
(12) D. Biddle, and T. Nordstrom, *Ark. Kemi.*, **32**, 359 (1970).
(13) B. Valeur, L. Monnerie, and J. P. Jarry, *J. Polym. Sci.*, submitted for publication.
(14) B. J. Hunt and J. G. Powles, *Proc. Phys. Soc., London*, **88**, 513 (1966).
(15) E. Helfand, *J. Chem. Phys.*, **54**, 4651 (1971).
(16) A. Abragam, "Principe du Magnetisme Nucléaire PUF Paris," 1961.
(17) T. M. Connor, "NMR Basic principles and Progress," Vol. 4, "Natural and Synthetic High Polymers," Springer-Verleg, Berlin, 1971.
(18) D. E. Woessner, *J. Chem. Phys.*, **37**, 647 (1962).
(19) J. H. Noggle and R. E. Schirmer, "The Nuclear Overhauser Effect," Academic Press, New York, N. Y., 1971.
(20) W. Anderson, "NMR and EPR Spectroscopy," Pergamon Press, New York, N. Y., 1960.
(21) J. P. Beyl, Thesis CNAM, Mulhouse, 1971.
(22) J. P. Kintzinger, Thèse, Strasbourg, 1970.
(23) P. J. Flory and J. E. Mark, *Makromol. Chem.*, **75**, 11 (1964).
(24) K. J. Liu and J. E. Anderson, *Macromolecules*, **3**, 163 (1970).
(25) A. Allerhand and R. K. Hailstone, *J. Chem. Phys.*, **56**, 3718 (1972).
(26) J. Schaefer, *Macromolecules*, **6**, 882 (1974).
(27) J. P. Cohen-Addad, *J. Chem. Phys.*, **60**, 2440 (1974).